

Myostatin knockout drives browning of white adipose tissue through activating the AMPK-PGC1 α -Fndc5 pathway in muscle

Tizhong Shan,^{*,1} Xinrong Liang,^{*,1} Pengpeng Bi,^{*} and Shihuan Kuang^{*,†,2}

^{*}Department of Animal Science and [†]Purdue University Center for Cancer Research, Purdue University, West Lafayette, Indiana, USA

ABSTRACT Myostatin (Mstn) is predominantly expressed in skeletal muscles and plays important roles in regulating muscle growth and development, as well as fat deposition. Mstn-knockout (*Mstn*^{-/-}) mice exhibit increased muscle mass due to both hypertrophy and hyperplasia, and leaner body composition due to reduced fat mass. Here, we show that white adipose tissue (WAT) of *Mstn*^{-/-} develops characteristics of brown adipose tissue (BAT) with dramatically increased expression of BAT signature genes, including *Ucp1* and *Pgc1 α* , and beige adipocyte markers *Tmem26* and *CD137*. Strikingly, the observed browning phenotype is non-cell autonomous and is instead driven by the newly defined myokine irisin (Fndc5) secreted from *Mstn*^{-/-} skeletal muscle. Within the muscle, *Mstn*^{-/-} leads to increased expression of AMPK and its phosphorylation, which subsequently activates PGC1 α and Fndc5. Together, our study defines a paradigm of muscle-fat crosstalk mediated by Fndc5, which is up-regulated and secreted from muscle to induce beige cell markers and the browning of WAT in *Mstn*^{-/-} mice. These results suggest that targeting muscle Mstn and its downstream signaling represents a therapeutic approach to treat obesity and type 2 diabetes.—Shan, T., Liang, X., Bi, P., Kuang, S. Myostatin knockout drives browning of white adipose tissue through activating the AMPK-PGC1 α -Fndc5 pathway in muscle. *FASEB J.* 27, 1981–1989 (2013). www.fasebj.org

Abbreviations: ActRIIB, activin receptor type IIB; AI, AMP-activated protein kinase inhibitor; AMPK, AMP-activated protein kinase; asWAT, anterior subcutaneous white adipose tissue; BAT, brown adipose tissue; BMP7, bone morphogenetic protein 7; Cidea, cell death-inducing DNA fragmentation factor, α subunit-like effector A; CM, conditioned medium; Fndc5, fibronectin type III domain containing 5; FBS, fetal bovine serum; H&E, hematoxylin and eosin; IHC, immunohistochemistry; ingWAT, inguinal white adipose tissue; Mstn, myostatin; PPAR α/γ , peroxisome proliferator-activated receptor α/γ ; PGC1 α/β , peroxisome proliferator-activated receptor coactivator 1 α/β ; Prdm16, PR domain containing 16; Prkaa1, protein kinase, AMP-activated, α 1 catalytic subunit; SVF, stromal-vascular fraction; TA, tibialis anterior; Tbx1, T-box 1; TGF β , transforming growth factor β ; Tmem26, transmembrane protein 26; UCP1, uncoupling protein 1; WAT, white adipose tissue; WT, wild type

Key Words: irisin • UCP1

ADIPOSE TISSUES PLAY critical roles in regulating energy metabolism and are thus closely associated with metabolic diseases, such as obesity and diabetes. In mammals, there are two main types of adipose tissues: white adipose tissue (WAT) and brown adipose tissue (BAT). WAT adipocytes are evolved to cope with food shortage by synthesizing and storing triglycerides as chemical energy. By contrast, BAT adipocytes contain numerous mitochondria with unique expression of uncoupling protein 1 (Ucp1), which burn chemical energy into heat to defend against hypothermia and obesity (1). Recently, a third type of adipocytes has been identified, so-called brite or beige adipocytes (2), which are found within WAT after cold exposure, chemical or hormonal stimulations, environment-elicited signaling from the central nervous system, and perturbed expression of key gene regulatory factors (3–16). Very recently, beige cells have been prospectively isolated from the WAT based on several cell surface markers, such as transmembrane protein 26 (Tmem26) and CD137 (17). Therefore, adipocytes can be broadly divided into white adipocytes, brown adipocytes, and adaptive beige adipocytes.

Myostatin (Mstn; also called GDF8), a member of the transforming growth factor β (TGF β) superfamily, is predominantly secreted by skeletal muscle to negatively affect muscle growth and development (18). *Mstn*^{-/-} mice have dramatically increased muscle mass, decreased fat deposition, improved insulin sensitivity, enhanced fatty acid oxidation, and increased resistance to obesity (19–21). Mstn also regulates the proliferation and differentiation of muscle stem cells and induces fiber-type switches (22–25).

Although Mstn is expressed at much lower levels in adipose tissues compared to muscles, multiple lines of

¹ These authors contributed equally to this work.

² Correspondence: 174B Smith Hall, 901 West State St., West Lafayette, IN 47907, USA. E-mail: skuang@purdue.edu
doi: 10.1096/fj.12-225755

This article includes supplemental data. Please visit <http://www.fasebj.org> to obtain this information.

evidence indicate that Mstn is involved in adipogenesis (26–28). Mstn inhibits the differentiation of brown adipocytes *in vitro* through the activin receptor IIB (ActRIIB)–Smad3 pathway (29, 30), and inhibition of Mstn promotes brown adipose phenotype in mice (21). By contrast, other TGF β signaling molecules and bone morphogenetic protein 7 (BMP7) promote BAT-like cells in WAT and skeletal muscles (5, 31, 32). Moreover, Mstn seems to inhibit the maturation of WAT preadipocytes, and aP2 lineage-specific overexpression of Mstn results in immature adipocytes with smaller cell size and increased thermogenesis and resistance to diet-induced obesity (27). However, given the low level of Mstn expression in adipose tissues, how Mstn exerts its effects on adipose tissue is unclear. In addition, whether *Mstn*^{-/-} affects the expression of beige cell-specific genes is unknown.

In the current study, we show that multiple WAT depots from *Mstn*^{-/-} mice express high levels of BAT and beige adipocyte signature genes. Notably, inhibition of Mstn signaling in WAT stromal-vascular fraction (SVF) cell cultures has no effect on the browning phenotype, suggesting that the effect of Mstn on WAT browning may be non-cell autonomous. Consistent with this notion, we show that *Mstn*^{-/-} muscle tissue extract and *Mstn*^{-/-} myotube conditioned medium (CM) both robustly induce browning of wild-type (WT) WAT SVF cells. Notably, the browning effect of *Mstn*^{-/-} CM can be abolished by a neutralizing antibody against irisin, pointing to a key role of this newly defined myokine in Mstn-mediated browning. Finally, we report that Mstn regulates muscle expression of irisin through the AMP-activated protein kinase (AMPK)–peroxisome proliferator-activated receptor coactivator 1 α (PGC1 α) pathway. Our results together demonstrate that Mstn is a critical factor in regulating a muscle myokine that induces browning of WAT.

MATERIALS AND METHODS

Animals

All procedures involving mice were performed in accordance with Purdue University's Animal Care and Use Committee. Mice were housed in the animal facility with free access to standard rodent chow and water. Mstn mutant (*Mstn*^{-/-}) mice were generated by Dr. S. E. Jin-Lee (The Johns Hopkins University, Baltimore, MD, USA) and previously described (18). Heterozygous *Mstn*^{+/-} mice were bred to generate *Mstn*^{-/-} and WT (*Mstn*^{+/+}) littermates that were used in this study. PCR genotyping was done using previously described protocols (24).

Muscle myoblast isolation and culture

Primary myoblasts were isolated using type I collagenase and dispase B digestion (33, 34). Briefly, hind-limb skeletal muscles from adult WT and *Mstn*^{-/-} mice were collected, minced, and digested. The digestions were stopped with Ham's F10 medium containing 20% fetal bovine serum (FBS), filtered (100 μ m), and centrifuged at 450 *g* for 5 min.

The resulting pellets were resuspended, and cells were seeded on collagen-coated dishes and cultured in growth medium containing Ham's F10 medium with 20% FBS, 4 ng/ml basic fibroblast growth factor, and 1% penicillin–streptomycin at 37°C with 5% CO₂. The medium was changed every 2 d. To prepare myotube CM, myoblasts from WT and *Mstn*^{-/-} mice were induced to differentiate in DMEM with 2% horse serum and 1% penicillin/streptomycin on 70% confluence. After 3 d of differentiation, cells were incubated in DMEM plus 10% FBS for 24 h; the resulting medium was then collected, filtered, and used as myotube CM. To inhibit Mstn signaling, cells were treated with anti-Mstn (kindly provided by Dr. Yong-Soo Kim, University of Hawaii, Manoa, HI, USA) or follistatin (SRP3045, 200 ng/ml; Sigma, St. Louis, MO, USA). To inhibit AMPK, cells were treated with compound C (5 μ M; Millipore, Billerica, MA, USA).

Adipose SVF cell isolation and culture

The WAT SVF cells were isolated using collagenase digestion followed by density separation (35, 36). Briefly, forelimb subcutaneous WAT depots were collected and minced into 2- to 5-mm² pieces. WAT pieces were then digested in 1.5 mg/ml collagenase at 37°C for 1.5–2 h. The digestions were stopped with DMEM containing 10% FBS, filtered (100 μ m), and centrifuged at 450 *g* for 5 min. The freshly isolated SVF cells from the WAT were seeded and cultured in growth medium containing DMEM, 20% FBS, and 1% penicillin/streptomycin at 37°C with 5% CO₂ for 3 d, followed by feeding with fresh medium every 2 d. On confluence, the cells were induced with induction medium containing DMEM, 10% FBS, 2.85 μ M insulin, 0.3 μ M dexamethasone, and 0.63 mM 3-isobutyl-methylxanthine (IBMX) for 3 d and then differentiated in differentiation medium containing DMEM, 200 nM insulin, and 10 nM T3 for 4 d until adipocytes matured. For fibronectin type III domain containing 5 (Fndc5) treatment, SVF cells were induced to differentiate, and Fndc5 peptide (ab117436, 20 nM; Abcam, Cambridge, MA, USA) was added in the differentiation medium during the last 2 d. For the CM treatment, SVF cells were induced to differentiate with 50% CM (1:1 CM: fresh induction medium) for 3 d and then matured in differentiation medium containing 50% CM for 4 d until adipocytes matured. For the Fndc5 antibody-neutralizing experiments, 1.25 μ g/ml of Fndc5 antibody (ab93373; Abcam) was used.

Plasma and muscle extract

Blood samples of anesthetized WT and *Mstn*^{-/-} mice were collected into EDTA-containing tubes to prevent coagulation. Samples were then centrifuged for 15 min at 3000 rpm, and the supernatant plasma were collected. For muscle extract, the gastrocnemius muscles of WT and *Mstn*^{-/-} mice were isolated and incubated in PBS with constant shaking for 1–2 h. Protein concentrations were measured using Pierce BCA Protein Assay Reagent (Pierce Biotechnology, Rockford, IL, USA), and equal amounts of plasma or muscle extracts from the WT and *Mstn*^{-/-} mice were used for all experiments.

Total RNA extraction, cDNA synthesis, and real-time PCR

Total RNA extraction, cDNA synthesis, and real-time PCR were performed as described previously (35, 36). Briefly, total RNA was extracted from cells using TRIzol reagent (Invitrogen, Carlsbad, CA, USA), according to the manufacturer's instructions. RNA was treated with RNase-free DNase I to remove contaminating genomic DNA. The purity and concentration of total RNA were measured by a

spectrophotometer (Nanodrop 3000; Thermo Fisher, Waltham, MA, USA) at 260 and 280 nm. Ratios of absorption (260/280 nm) of all samples were between 1.8 and 2.0. Then 5 μg of total RNA was reversed transcribed using random hexaprimers and Moloney murine leukemia virus (M-MLV) reverse transcriptase. Real-time PCR was carried out with a Roche LightCycler 480 PCR system with SYBR Green Master Mix and gene-specific primers (Roche Diagnostics, Indianapolis, IN, USA). Primer sequences are from published papers (17, 35, 36). The $2^{-\Delta\Delta CT}$ method was used to analyze the relative expression of genes using 18S rRNA as an internal control.

Protein extraction and Western blot analysis

The protein extraction and Western blot procedures were conducted as described previously (36). Briefly, total protein was isolated from cells using RIPA buffer containing 50 mM Tris-HCl (pH 8.0), 150 mM NaCl, 1% Nonidet P-40, 0.5% sodium deoxycholate and 0.1% SDS. Protein concentrations were determined using Pierce BCA protein assay reagent (Pierce Biotechnology). Proteins were separated by SDS-PAGE, transferred onto PVDF membranes (Millipore Corp., Billerica, MA, USA), and blocked in 5% fat-free milk for 1 h at room temperature, then incubated with primary antibodies in 5% milk overnight at 4°C. The Ucp1 and Fndc5 antibodies were from Abcam, and Pgc1 α , pAMPK, GAPDH, and α -tubulin were from Santa Cruz Biotechnology (Santa Cruz, CA, USA). Secondary antibodies (anti-rabbit IgG or anti-mouse IgG; Jackson ImmunoResearch, West Grove, PA, USA) were diluted 1:8000. Immunodetection was performed using enhanced chemiluminescence (ECL) Western blotting substrate (Pierce Biotechnology) and detected with a Gel Logic 2200 imaging system (Carestream, Rochester, NY, USA).

Hematoxylin and eosin (H&E) and immunohistochemistry (IHC) staining

WAT tissues from the WT and *Mstn*^{-/-} mice were fixed in 10% formalin for 24–48 h at room temperature. Fixed tissues were embedded in paraffin and cut at 3–10 μm for H&E and IHC staining. For H&E staining, the sections were deparaffinized, rehydrated, and stained with hematoxylin for 15 min. Sections were then rinsed in running tap water and stained with eosin for 1 min. H&E-stained sections were dehydrated and mounted. For IHC staining, tissue sections were blocked with PBS containing 5% goat serum, 2% bovine serum albumin (BSA), 0.2% Triton X-100, and 0.1% sodium azide for 1 h after antigen retrieval. Then, the samples were incubated with Ucp1 primary antibodies diluted in blocking buffer overnight. After washing with PBS, the samples were incubated with secondary antibodies for 45 min at room temperature, followed by reactions with ABC and DAB reagents. Images were captured with a Nikon D90 digital camera installed on a Nikon (Diaphot) inverted microscope (Nikon, Tokyo, Japan).

Data analysis

All experimental data are presented as means \pm SE. Comparisons were made by unpaired 2-tailed Student's *t* tests or 1-way ANOVA, as appropriate. Effects were considered significant at $P < 0.05$.

RESULTS

Mstn knockout induces browning of WAT

To examine whether Mstn affects adipogenesis and WAT browning, we utilized the *Mstn*^{-/-} mice, which exhibit increased muscle mass and reduced fat mass (Fig. 1A), as previously reported (37). Compared to WT WAT, *Mstn*^{-/-} anterior subcutaneous WAT (asWAT) and inguinal WAT (ingWAT) appeared much browner in color (Fig. 1A, B), suggesting browning of *Mstn*^{-/-} WAT. Indeed, H&E staining revealed that compared to WT ingWAT, which mostly consists of large-sized adipocytes with unilocular lipid droplets (Fig. 1C), *Mstn*^{-/-} ingWAT contained numerous small-sized brown adipocyte-like cells filled with multilocular small lipid droplets (Fig. 1D). Immunohistochemistry staining showed that the Ucp1 immunoreactivity signal was much stronger in *Mstn*^{-/-} WAT than in WT WAT (Fig. 1E, F). Quantitative PCR (qPCR) and Western blot

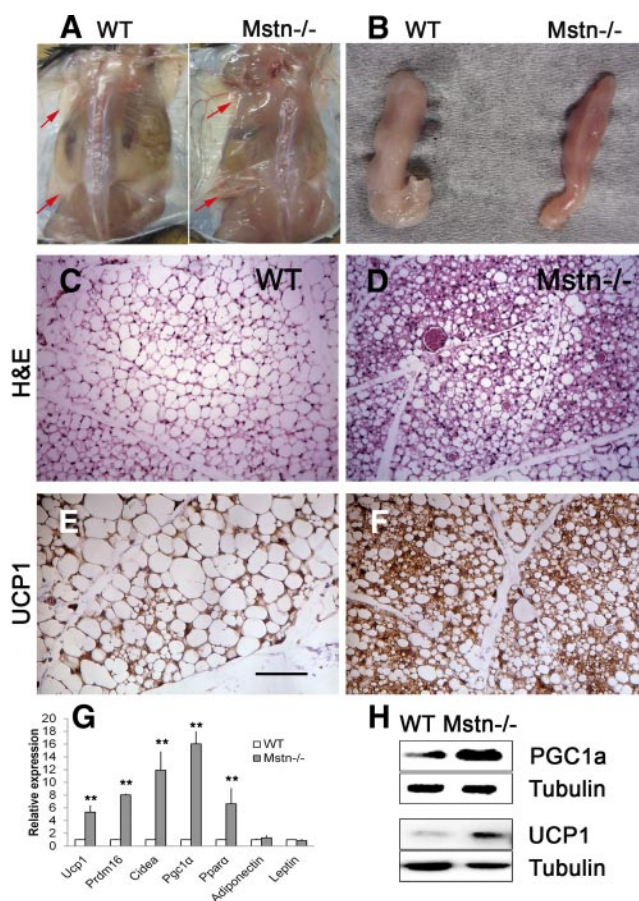


Figure 1. Mstn knockout induces browning of WAT. A) Dorsal view of WT and *Mstn*^{-/-} mice. Red arrows indicate the anterior subcutaneous WAT (asWAT) and inguinal WAT (ingWAT). B) Representative image of WT and *Mstn*^{-/-} ingWAT. C, D) H&E staining of control and *Mstn*^{-/-} ingWAT. E, F) Ucp1 immunoreactivity signal (brown) of WT and *Mstn*^{-/-} ingWAT. G) Relative expression of BAT- and WAT-specific genes in the WT and *Mstn*^{-/-} ingWAT. H) Western blotting image showing UCP1 and PGC1 α expression of WT and *Mstn*^{-/-} ingWAT. Error bars = SE; $n = 6$. ** $P < 0.01$.

analysis further confirmed that compared to the WT WAT, *Mstn*^{-/-} WAT expressed elevated levels of BAT signature markers *Ucp1*, *Pgc1α*, PR domain containing 16 (*Prdm16*), cell death-inducing DNA fragmentation factor, α subunit-like effector A (*Cidea*), and peroxisome proliferator-activated receptor α (*PPARα*) but not WAT markers *adiponectin* and *leptin* (Fig. 1G, H). Similar results were found in multiple subcutaneous WAT depots. These data demonstrate that lack of *Mstn* robustly induces browning of subcutaneous WAT.

One way that browning of WAT occurs is mediated by a population of beige (brite) adipocytes that uniquely express several signature genes, including *Tmem26*, *CD137*, and T-box 1 (*Tbx1*) (17). Consistent with the browning phenotype, *Mstn*^{-/-} WAT also expressed higher levels of *Tmem26* and *CD137* in both asWAT and ingWAT depots (Supplemental Fig. S1A, B). To examine whether the increased beige adipocyte marker expression in the adipose tissue is due to increases in beige cell progenitors in *Mstn*^{-/-} WAT, we isolated from asWAT and ingWAT the SVFs that are known to contain preadipocytes but not mature adipocytes. However, there was no significant difference in the expression of *Tmem26* and *CD137* between the *Mstn*^{-/-} and WT SVF cells (Supplemental Fig. S1C, D). These results indicate that *Mstn*^{-/-} up-regulates beige adipocyte marker expression in mature adipocytes but not preadipocytes.

Inhibition of *Mstn* signaling fails to induce browning of white adipocytes *in vitro*

We next sought to determine whether browning is an autonomous effect of inhibition of *Mstn* signaling in the adipocytes. We induced adipogenic differentiation of WAT SVF cells isolated from WT and *Mstn*^{-/-} mice, and assessed expression of BAT marker genes. The *Mstn*^{-/-} SVF cells were able to differentiate normally into lipid-filling adipocytes without obvious morphological defects. Surprisingly, adipocytes differentiated from WT and *Mstn*^{-/-} SVF cells expressed similar levels of *Ucp1*, *Prdm16*, *Cidea*, *Pgc1α*, and *Pparα* (Supplemental Fig. S2A). To confirm these results, we induced adipogenic differentiation of WAT SVF cells from WT mice in the presence of soluble ActRIIB (sActRIIB; 2000 ng/ml) or a neutralizing antibody against *Mstn* (anti-*Mstn*; 2000 ng/ml), agents that have been shown to inhibit *Mstn* signaling (24). Neither treatment affected the overall differentiation of the SVF cells or induced BAT-specific genes after differentiation (Supplemental Fig. S2B, C). Taken together, these data demonstrate that loss of *Mstn* or inhibition of *Mstn* signaling in preadipocytes does not account for the browning phenotype observed in the WAT of *Mstn*^{-/-} mice.

Skeletal muscle-derived factor drives WAT browning in *Mstn*^{-/-} mice

The non-cell-autonomous effect of *Mstn* on the browning of WAT adipocytes suggests that one or more

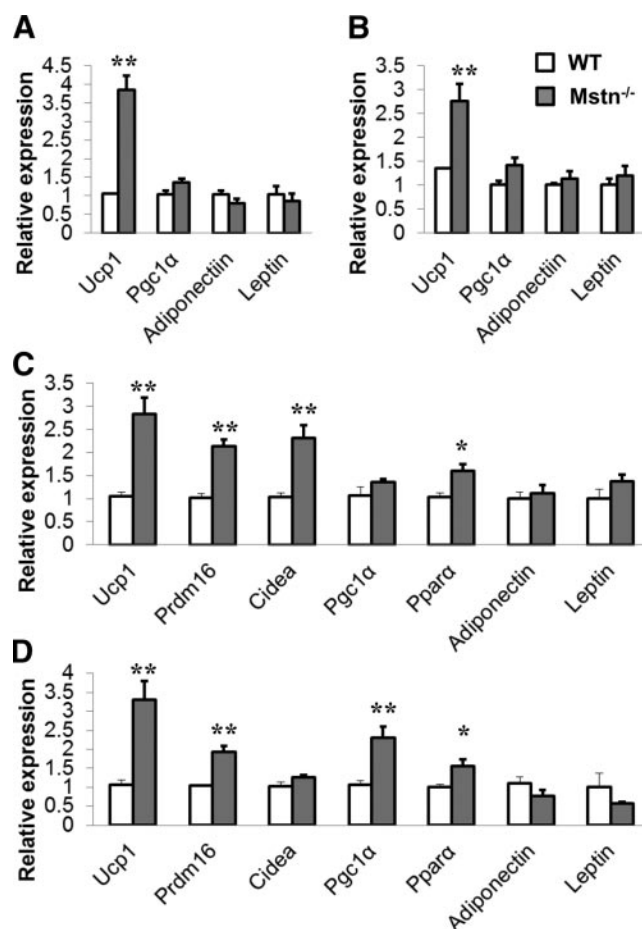


Figure 2. Muscle-derived factors induce browning of white adipocytes. A) Relative expression of BAT (*Ucp1*) and WAT (*adiponectin*, *leptin*) marker genes in white adipocytes differentiated from ingWAT and treated with plasma derived from WT or *Mstn*^{-/-} mice; *n* = 4. B) Relative expression of BAT and WAT marker genes in white adipocytes differentiated from ingWAT and treated with WT or *Mstn*^{-/-} muscle extracts; *n* = 6. C, D) Relative expression of BAT and WAT marker genes in asWAT-derived (C) and visceral WAT-derived (D) adipocytes treated with WT and *Mstn*^{-/-} myotube CM; *n* = 6. **P* < 0.05; ***P* < 0.01.

circulating factors might be responsible for this process. Indeed, we found that plasma extracted from *Mstn*^{-/-} mouse blood potentially unregulated *Ucp1* expression in adipocytes differentiated from WAT SVF cells of WT mice (Fig. 2A). We hypothesize that a muscle-derived factor (myokine) regulates the browning of WAT in the *Mstn*^{-/-} mice, based on the inversely correlated increases in muscle mass and decreases in fat mass in these mice. As expected from this hypothesis, *Mstn*^{-/-} skeletal muscle extracts significantly up-regulated *Ucp1* expression in adipocytes differentiated from WAT SVF cells of WT mice (Fig. 2B). As whole-muscle extracts contain many non-muscle-derived factors, we next directly tested the effect of CM collected from myotube cultures differentiated from WT and *Mstn*^{-/-} myoblasts (designated as WT-CM and *Mstn*^{-/-}-CM). Compared with the WT-CM, *Mstn*^{-/-}-CM significantly increased expression of BAT marker genes *Ucp1*,

Prdm16, *Cidea*, and *Pparα*, but not WAT marker genes *adiponectin* and *leptin*, in subcutaneous WAT SVF-derived adipocytes (Fig. 2C). Similar changes were observed using visceral WAT-derived SVF cells treated with WT-CM or *Mstn*^{-/-}-CM (Fig. 2D). These results indicate that browning of WAT in *Mstn*^{-/-} mice is muscle driven.

Muscle-derived Fndc5 (irisin) mediates browning of WAT in *Mstn*^{-/-} mice

A newly identified myokine, irisin (encoded by the *Fndc5* gene), has been reported to mediate exercise-induced browning of WAT (3). We confirmed that *Fndc5* is highly expressed in muscle compared to WAT (>200-fold higher in muscle). To investigate whether the browning in *Mstn*^{-/-} mice is mediated by irisin, we first checked the expression of *Fndc5* in WT and *Mstn*^{-/-} muscles. The mRNA levels of *Fndc5*, along with its upstream activators *Pgc1α* and *Pgc1β*, were up-regulated ~3 fold in the *Mstn*^{-/-} than WT muscles (Fig. 3A). In addition, the protein levels of *Fndc5* and *Pgc1α* were also elevated in the *Mstn*^{-/-} compared to WT muscles (Fig. 3B, C). Furthermore, inhibition of

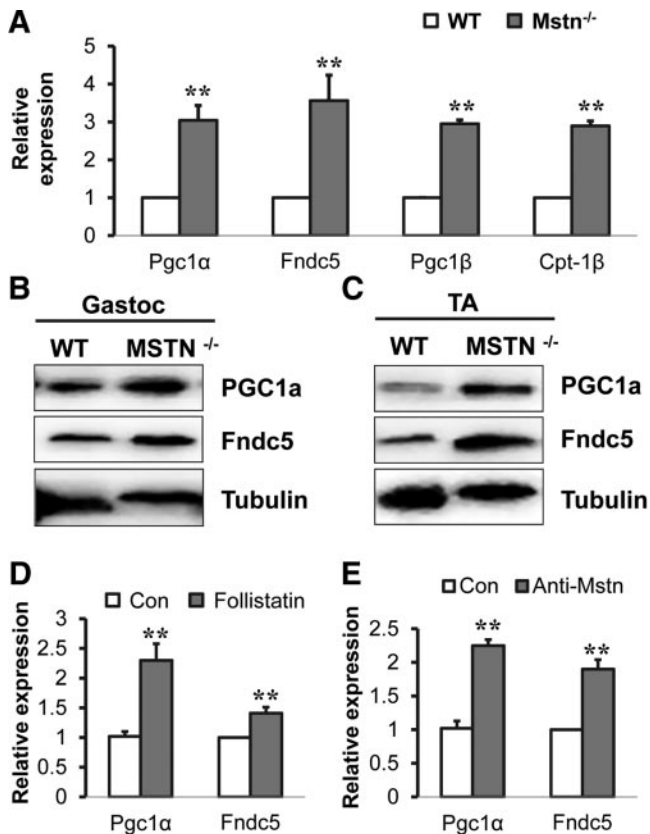


Figure 3. Inhibition of Mstn increases the expression of *Pgc1α* and *Fndc5* in muscle. *A*) Relative expression of *Pgc1α*, *Fndc5*, *Pgc1β*, and *Cpt1β* in WT and *Mstn*^{-/-} tibialis anterior (TA) muscles. *B*, *C*) PGC1α and *Fndc5* protein levels in the gastrocnemius (gastoc; *B*) and TA (*C*) muscles of WT and *Mstn*^{-/-} mice. *D*, *E*) Relative expression of *Pgc1α* and *Fndc5* in myotubes treated with follistatin (*D*) or Mstn antibody (*E*). ***P* < 0.01; *n* = 4.

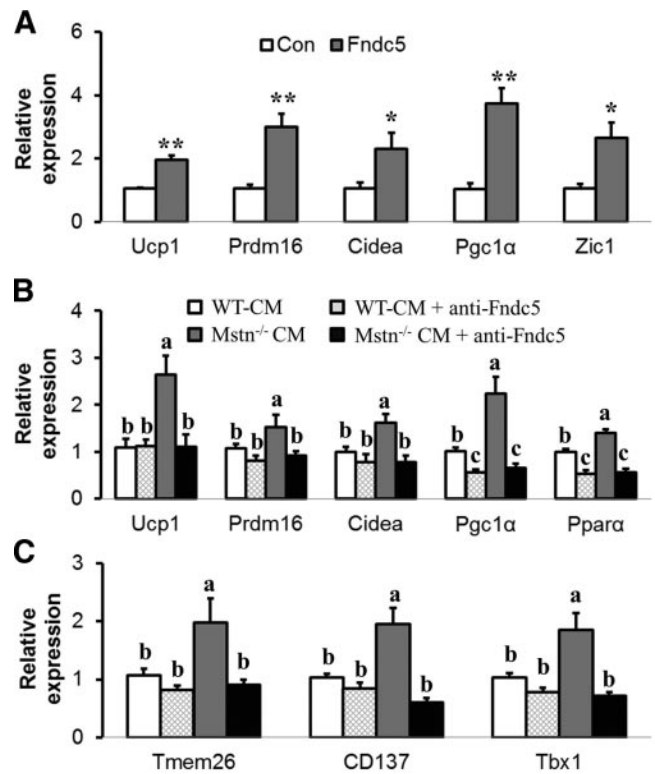


Figure 4. Muscle-derived *Fndc5* mediates browning of WAT in the *Mstn*^{-/-} mice. *A*) *Fndc5*-recombinant protein (20 nM) induces expression of BAT marker genes in white adipocyte cultures; *n* = 4. **P* < 0.05, ***P* < 0.01. *B*) Relative expression of BAT marker genes in white adipocytes treated with WT myotube CM (WT-CM), WT myotube CM plus *Fndc5* antibody (1.25 μg/ml, WT-CM + anti-*Fndc5*), *Mstn*^{-/-} myotube CM (MSTN-CM), and *Mstn*^{-/-} myotube CM plus *Fndc5* antibody (1.25 μg/ml, MSTN-CM + anti-*Fndc5*); *n* = 6. Note that *Fndc5* antibody abolishes the effect of *Mstn*^{-/-} myotube CM on browning. *C*) Relative expression of beige adipocyte-specific genes in white adipocytes treated as indicated in *B*; *n* = 6. ^{a,b,c} Bars with no letter in common differ significantly.

Mstn signaling with anti-*Mstn* antibody or follistatin (200 ng/ml) both up-regulated the expression of *Pgc1α* and *Fndc5* in cultured myotubes (Fig. 3D, E). Collectively, these results show that *Mstn*^{-/-} increases *Pgc1α* and *Fndc5* expression in the skeletal muscle.

We further investigated whether irisin is the key active component in *Mstn*^{-/-} myotube conditioned medium that induce browning of WAT adipocytes. We first confirmed that *Fndc5* recombinant peptide robustly induces expression of BAT marker genes (*Ucp1*, *Prdm16*, *Cidea*, and *Pgc1α*) in adipocytes differentiated from WAT SVF cells (Fig. 4A). We next used *Fndc5* antibody to neutralize the irisin in *Mstn*^{-/-}-CM. The addition of anti-*Fndc5* to WT myotube-conditioned medium (WT-CM) had no effect on the expression of *Ucp1*, *Prdm16*, and *Cidea*, but moderately reduced the expression of *Pgc1α* and *Pparα* (Fig. 4B). This result suggests that WT-CM contains little irisin. Consistent with our earlier results in Fig. 2C, *Mstn*^{-/-}-CM up-regulated all the BAT signature genes of cultured adipocytes (Fig. 4B). Most importantly, anti-*Fndc5* abolished the browning effects of *Mstn*^{-/-}-CM (Fig. 4B),

demonstrating that irisin is the active component in the *Mstn*^{-/-}-CM that induces browning. Furthermore, anti-Fndc5 also abolished the inductive effect of *Mstn*^{-/-}-CM on beige adipocyte markers *Tmem26*, *CD137* and *Tbx1* (Fig. 4C). These results provide compelling evidence that *Mstn*^{-/-} drives browning of WAT through muscle-specific irisin.

Mstn^{-/-} activates the AMPK-PGC1 α -Fndc5 pathway in muscle

Lastly, we investigated the molecular pathway through which *Mstn*^{-/-} up-regulates Fndc5 in muscle. We detected increased amount of total AMPK and the activated (phosphorylated) pAMPK in both tibialis anterior (TA) and gastrocnemius muscles of *Mstn*^{-/-} compared to WT mice (Fig. 5A, B). In agreement with these *in vivo* results, inhibition of Mstn signaling by anti-Mstn or follistatin significantly up-regulated the expression of protein kinase, AMP-activated, α 1 catalytic subunit

(*Prkaa1*; encoding AMPK subunit 1) in cultured myoblasts (Fig. 5C, D). To examine whether AMPK is sufficient and necessary to mediate the effect of Mstn on Pgc1 α and Fndc5, we utilized AMPK inhibitor (AI) combined with Mstn inhibition. AI alone (5 μ M) significantly reduced, whereas anti-Mstn up-regulated, the mRNA levels of *Pgc1 α* and *Fndc5* in cultured myoblasts (Fig. 5E, F). Notably, inhibition of AMPK abolished the effects of anti-Mstn on the expression of *Pgc1 α* and *Fndc5* (Fig. 5E, F). In summary, our results demonstrate that *Mstn*^{-/-} activates the AMPK-PGC1 α -Fndc5 pathway in muscle, leading to increased production of irisin that induces browning of WATs.

DISCUSSION

Obesity, caused by accumulations of WAT due to imbalanced energy expenditure, is an increasingly serious worldwide health concern. One strategy to fight against obesity is to transform energy-storing white adipocytes into heat-producing beige adipocytes in WAT, a process called browning (19, 38). Our finding that *Mstn*^{-/-} adipose tissue exhibits browning phenotype is consistent with a recent report (21) and pointing to the possibility of inhibiting Mstn signaling to treat obesity. Mstn is a member of the TGF β superfamily, which has been implicated in regulating brown fat phenotype. For example, TGF β /Smad3 signaling regulates brown adipocytes induction in WAT (12, 29, 32). In addition, BMP7, another member of the TGF β superfamily, also induces brown adipogenesis (5, 31). By contrast, our results that Mstn knockout promotes browning suggest that Mstn signaling inhibits browning. In support of our results, a recent study demonstrates that Mstn inhibits brown adipocyte differentiation *via* regulation of Smad3-mediated β -catenin stabilization (29, 30). Our current study and previous study together suggest that different members of the TGF β superfamily have distinct functions in brown adipogenesis (39). This notion is consistent with the well-documented broad and sometimes opposing functions of the TGF β superfamily members (39). Future studies should elucidate how different types of TGF β signaling differentially regulate white and brown adipocytes.

We show that *Mstn*^{-/-}-mediated browning of WAT is non-cell autonomous, and inhibition of Mstn signaling had no effect on the differentiation and fate (white *vs.* brown) determination of WAT SVF cells. This is probably due to the low levels of Mstn expression in WAT and does not exclude the possibility that high levels of Mstn can affect adipogenesis. Although previous studies indicate that overexpression of Mstn or activation of Mstn signaling inhibits both white and brown adipocyte differentiation (27, 30), the physiological relevance of such results is uncertain due to the low levels of endogenous Mstn expression in white adipocytes. Our results are consistent with those by Guo *et al.* (37) showing that inhibition of Mstn through transgenic overexpression of ActRIIB specifically in WAT had no effect on body com-

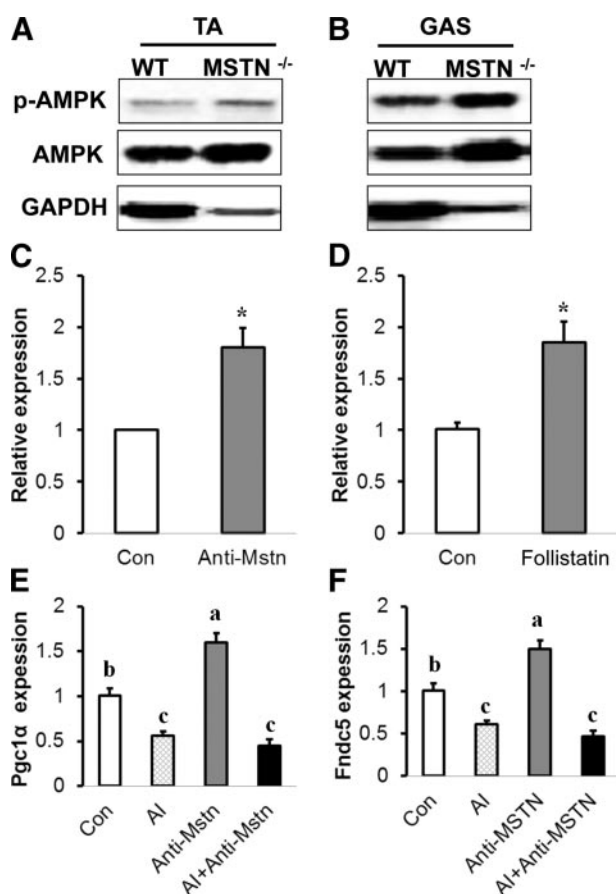


Figure 5. Inhibition of Mstn up-regulates Pgc1 α and Fndc5 through AMPK pathway. A, B) Relative levels of total AMPK and phosphorylated pAMPK in WT and *Mstn*^{-/-} TA (A) and gastrocnemius (gas; B) muscles. C, D) Relative expression of *Prkaa1* in myoblast treated with Mstn antibody (C) or follistatin (D). **P* < 0.05; *n* = 4. E, F) AMPK inhibitor (AI; compound C, 5 μ M) abolishes the effect of the anti-Mstn on the expression of *Pgc1 α* (E) and *Fndc5* (F) in cultured myotubes. ^{a,b,c}Bars with no letter in common differ significantly; *n* = 4.

position, glucose, and insulin tolerance in mice. Thus, the browning of WAT in *Mstn*^{-/-} mice is due to the deletion of Mstn in muscle or other organs.

We provide several lines of evidence to support that a muscle-secreted cue leads to browning in the *Mstn*^{-/-} mice. First, *Mstn*^{-/-} whole-muscle extract and myotube CM robustly induces browning of white adipocytes. Second, *Mstn*^{-/-} up-regulates the expression of Fndc5 (irisin) in the muscle. Third, Fndc5 recombinant protein alone is sufficient to induce browning of white adipocytes. Fourth, and most important, neutralization of Fndc5 abolishes the browning effect of *Mstn*^{-/-} myotube CM. These results not only confirm previous speculation that hypertrophic muscle induces browning of adipose tissue (19) but further identify Fndc5 as the muscle-derived browning signal. Our results are consistent with recent seminal studies demonstrating that irisin plays important roles in stimulating Ucp1 expression and browning of WAT (3, 17, 38). Irisin is the protein product of Fndc5 gene, which encodes a type I membrane protein whose extracellular domain is proteolytically cleaved to form irisin (3). Exercise and Pgc1 α overexpression induce Fndc5 gene expression in muscle and subsequently increase the concentration of circulating irisin. Once released from muscle, irisin circulates as a hormone to exert its function to induce browning of WAT and activate oxygen consumption and thermogenesis in white adipocytes (3, 38). Future studies using muscle-specific *Mstn*-knock-out mice should provide direct insights into the role of Mstn in WAT browning.

Although our study identifies muscle-specific irisin as a factor that mediates the browning of WAT in *Mstn*^{-/-} mice, our result does not rule out the possibility that other players may also be involved. *Mstn*^{-/-} mice have reduced blood insulin and glucose levels and increased insulin sensitivity, and are protected from high-fat diet-induced obesity (37). Inhibition of Mstn further reverses the diabetic phenotype in a mouse model (40). Interestingly, genetic prevention of chronic hyperinsulinemia through *Ins2* null and *Ins1* haploinsufficiency not only blocks high-fat diet-induced obesity but, strikingly, also reprograms white adipocytes into brown adipocyte-like cells (41). These reprogrammed white adipocytes express high levels of UCP1 and exhibit elevated energy expenditure (41). Therefore, systemic improvements of insulin sensitivity in the *Mstn*^{-/-} mice may also contribute to the observed browning phenotype.

Notably, we illustrate the molecular pathway through which *Mstn*^{-/-} up-regulates Fndc5 expression in the muscle. We show that *Mstn*^{-/-} and inhibition of Mstn signaling with anti-Mstn or follistatin all increase the expression of Pgc1 α , an upstream activator of Fndc5 (3). Consistently, previous studies have indicated that inhibition of Mstn and exercise increase mRNA and protein levels of Pgc1 α in the skeletal muscle (42, 43). In addition, it has been shown that there are higher levels of Pgc1 α expression in *Mstn*^{-/-} muscle (44). We further show that *Mstn*^{-/-} activates AMPK, a Pgc1 α

activator, in muscles. Similarly, inhibition of Mstn signaling with anti-Mstn or follistatin up-regulated *Prkaa1* expression in cultured myoblasts. The observed modest effect (<2-fold increase) of Mstn inhibition in cultured myoblasts may be due to their undifferentiated state. More critically, we show that the effects of anti-Mstn on the expression of Pgc1 α and Fndc5 are abolished by AI, thus suggesting that AMPK activation is necessary to mediate the effect of Mstn on Pgc1 α and Fndc5 expression. Together, our study establishes that the AMPK–Pgc1 α –Fndc5 axis in the muscle mediate the browning effect of *Mstn*^{-/-} mice.

At present, it is unclear how mutation of Mstn leads to up-regulation of AMPK and its activation in muscle. Several potential mechanisms can be involved. It has been reported that *Mstn*^{-/-} leads to muscle fiber-type switching toward fast myosin heavy-chain isoforms (24, 45, 46). As fast myofibers mostly utilize glycolytic metabolic pathways and contract much faster, the ratio of AMP/ATP should be increased, with fiber-type switching toward fast myofibers, leading to more robust activation of AMPK (47). In addition, *Mstn*^{-/-}-induced fiber-type switching may also lead to increases in the expression of AMPK α 1, γ 2, and γ 3 subunits, known to be expressed at higher levels in fast than slow myofibers (47, 48). Furthermore, it has been well documented that activation of ActRIIB by Mstn inhibits phosphorylation of Akt, a key activator of the mTOR pathway involved in protein synthesis and inhibitor of FoxO1 that promotes protein degradation (37, 49, 50). Thus, *Mstn*^{-/-} should increase protein synthesis and decrease protein degradation, resulting in overall increase of muscle proteins, including AMPK. Finally, *Mstn*^{-/-} may activate or increase the level of LKB1, an upstream activator of AMPK. Future studies should address these possibilities.

In summary, our present study elucidates a signaling pathway activated by mutation of Mstn that drives browning of WAT. We show that browning of WAT in the *Mstn*^{-/-} mice is not a direct effect of Mstn deletion in WAT, but an indirect effect from a myokine that is regulated by Mstn and its downstream signaling cascade (AMPK-PGC1 α -Fndc5). These results enhance our understanding of the function of Mstn and further suggest that Mstn signaling represent a promising therapeutic target to treat obesity and its associated diabetes. **[F]**

This project is partially supported by funding from the Muscular Dystrophy Association, the U.S. National Institutes of Health, and the U.S. Department of Agriculture to S.K. The authors thank Yong-Soo Kim (University of Hawaii, Manoa, HI, USA) for providing anti-Mstn and ActRIIB. The authors are grateful to Jun Wu and Pengpeng Zhang for mouse colony and technical support. The authors declare no conflicts of interests.

REFERENCES

1. Cannon, B., and Nedergaard, J. (2004) Brown adipose tissue: function and physiological significance. *Physiol. Rev.* **84**, 277–359
2. Walden, T. B., Hansen, I. R., Timmons, J. A., Cannon, B., and Nedergaard, J. (2012) Recruited vs. nonrecruited molecular

- signatures of brown, "brite," and white adipose tissues. *Am. J. Physiol. Endocrinol. Metab.* **302**, E19–E31
3. Bostrom, P., Wu, J., Jedrychowski, M. P., Korde, A., Ye, L., Lo, J. C., Rasbach, K. A., Bostrom, E. A., Choi, J. H., Long, J. Z., Kajimura, S., Zingaretti, M. C., Vind, B. F., Tu, H., Cinti, S., Hojlund, K., Gygi, S. P., and Spiegelman, B. M. (2012) A PGC1- α -dependent myokine that drives brown-fat-like development of white fat and thermogenesis. *Nature* **481**, 463–468
 4. Fisher, F. M., Kleiner, S., Douris, N., Fox, E. C., Mepani, R. J., Verdeguer, F., Wu, J., Kharitonov, A., Flier, J. S., Maratos-Flier, E., and Spiegelman, B. M. (2012) FGF21 regulates PGC-1 α and browning of white adipose tissues in adaptive thermogenesis. *Genes Dev.* **26**, 271–281
 5. Tseng, Y. H., Kokkoto, E., Schulz, T. J., Huang, T. L., Winnay, J. N., Taniguchi, C. M., Tran, T. T., Suzuki, R., Espinoza, D. O., Yamamoto, Y., Ahrens, M. J., Dudley, A. T., Norris, A. W., Kulkarni, R. N., and Kahn, C. R. (2008) New role of bone morphogenetic protein 7 in brown adipogenesis and energy expenditure. *Nature* **454**, 1000–1004
 6. Ohno, H., Shinoda, K., Spiegelman, B. M., and Kajimura, S. (2012) PPAR γ agonists induce a white-to-brown fat conversion through stabilization of PRDM16 protein. *Cell Metab.* **15**, 395–404
 7. Cao, L., Choi, E. Y., Liu, X., Martin, A., Wang, C., Xu, X., and Durning, M. J. (2011) White to brown fat phenotypic switch induced by genetic and environmental activation of a hypothalamic-adipocyte axis. *Cell Metab.* **14**, 324–338
 8. Powelka, A. M., Seth, A., Virbasius, J. V., Kiskinis, E., Nicoloso, S. M., Guilherme, A., Tang, X., Straubhaar, J., Cherniack, A. D., Parker, M. G., and Czech, M. P. (2006) Suppression of oxidative metabolism and mitochondrial biogenesis by the transcriptional corepressor RIP140 in mouse adipocytes. *J. Clin. Invest.* **116**, 125–136
 9. Qiang, L., Wang, L., Kon, N., Zhao, W., Lee, S., Zhang, Y., Rosenbaum, M., Zhao, Y., Gu, W., Farmer, S. R., and Accili, D. (2012) Brown remodeling of white adipose tissue by SirT1-dependent deacetylation of PPAR γ . *Cell* **150**, 620–632
 10. Scime, A., Grenier, G., Huh, M. S., Gillespie, M. A., Bevilacqua, L., Harper, M. E., and Rudnicki, M. A. (2005) Rb and p107 regulate preadipocyte differentiation into white versus brown fat through repression of PGC-1 α . *Cell Metab.* **2**, 283–295
 11. Seale, P., Conroe, H. M., Estall, J., Kajimura, S., Frontini, A., Ishibashi, J., Cohen, P., Cinti, S., and Spiegelman, B. M. (2011) Prdm16 determines the thermogenic program of subcutaneous white adipose tissue in mice. *J. Clin. Invest.* **121**, 96–105
 12. Yadav, H., and Rane, S. G. (2012) TGF- β /Smad3 signaling regulates brown adipocyte induction in white adipose tissue. *Front. Endocrinol. (Lausanne)* **3**, 35
 13. Madsen, L., Pedersen, L. M., Lillefosse, H. H., Fjaere, E., Bronstad, I., Hao, Q., Petersen, R. K., Hallenborg, P., Ma, T., De Matteis, R., Araujo, P., Mercader, J., Bonet, M. L., Hansen, J. B., Cannon, B., Nedergaard, J., Wang, J., Cinti, S., Voshol, P., Daskalakis, S. O., and Kristiansen, K. (2010) UCP1 induction during recruitment of brown adipocytes in white adipose tissue is dependent on cyclooxygenase activity. *PLoS One* **5**, e11391
 14. Cederberg, A., Gronning, L. M., Ahren, B., Tasken, K., Carlsson, P., and Enerback, S. (2001) FOXC2 is a winged helix gene that counteracts obesity, hypertriglyceridemia, and diet-induced insulin resistance. *Cell* **106**, 563–573
 15. Picard, F., Gehin, M., Annicotte, J. S., Rocchi, S., Champy, M. F., O'Malley, B. W., Chambon, P., and Auwerx, J. (2002) SRC-1 and TIF2 control energy balance between white and brown adipose tissues. *Cell* **111**, 931–941
 16. Tsukiyama-Kohara, K., Poulin, F., Kohara, M., DeMaria, C. T., Cheng, A., Wu, Z. D., Gingras, A. C., Katsume, A., Elchebly, M., Spiegelman, B. M., Harper, M. E., Tremblay, M. L., and Sonenberg, N. (2001) Adipose tissue reduction in mice lacking the translational inhibitor 4E-BP1. *Nat. Med.* **7**, 1128–1132
 17. Wu, J., Bostrom, P., Sparks, L. M., Ye, L., Choi, J. H., Giang, A. H., Khandekar, M., Virtanen, K. A., Nuutila, P., Schaart, G., Huang, K., Tu, H., van Marken Lichtenbelt, W. D., Hoeks, J., Enerback, S., Schrauwen, P., and Spiegelman, B. M. (2012) Beige adipocytes are a distinct type of thermogenic fat cell in mouse and human. *Cell* **150**, 366–376
 18. McPherron, A. C., Lawler, A. M., and Lee, S. J. (1997) Regulation of skeletal muscle mass in mice by a new TGF- β superfamily member. *Nature* **387**, 83–90
 19. Lebrasseur, N. K. (2012) Building muscle, browning fat and preventing obesity by inhibiting myostatin. *Diabetologia* **55**, 13–17
 20. Bernardo, B. L., Wachtmann, T. S., Cosgrove, P. G., Kuhn, M., Opsahl, A. C., Judkins, K. M., Freeman, T. B., Hadcock, J. R., and Lebrasseur, N. K. (2010) Postnatal PPAR delta activation and myostatin inhibition exert distinct yet complementary effects on the metabolic profile of obese insulin-resistant mice. *PLoS One* **5**
 21. Zhang, C., McFarlane, C., Lokireddy, S., Masuda, S., Ge, X., Gluckman, P. D., Sharma, M., and Kambadur, R. (2012) Inhibition of myostatin protects against diet-induced obesity by enhancing fatty acid oxidation and promoting a brown adipose phenotype in mice. *Diabetologia* **55**, 183–193
 22. Joulia, D., Bernardi, H., Garandel, V., Rabenoelina, F., Vernus, B., and Cabello, G. (2003) Mechanisms involved in the inhibition of myoblast proliferation and differentiation by myostatin. *Exp. Cell Res.* **286**, 263–275
 23. Thomas, M., Langley, B., Berry, C., Sharma, M., Kirk, S., Bass, J., and Kambadur, R. (2000) Myostatin, a negative regulator of muscle growth, functions by inhibiting myoblast proliferation. *J. Biol. Chem.* **275**, 40235–40243
 24. Wang, M., Yu, H., Kim, Y. S., Bidwell, C. A., and Kuang, S. H. (2012) Myostatin facilitates slow and inhibits fast myosin heavy-chain expression during myogenic differentiation. *Biochem. Biophys. Res. Co.* **426**, 83–88
 25. McCroskery, S., Thomas, M., Maxwell, L., Sharma, M., and Kambadur, R. (2003) Myostatin negatively regulates satellite cell activation and self-renewal. *J. Cell Biol.* **162**, 1135–1147
 26. Artaza, J. N., Bhasin, S., Magee, T. R., Reisz-Porszasz, S., Shen, R. Q., Groome, N. P., Fareez, M. M., and Gonzalez-Cadavid, N. F. (2005) Myostatin inhibits myogenesis and promotes adipogenesis in C3H 10T (1/2) mesenchymal multipotent cells. *Endocrinology* **146**, 3547–3557
 27. Feldman, B. J., Streeper, R. S., Farese, R. V., and Yamamoto, K. R. (2006) Myostatin modulates adipogenesis to generate adipocytes with favorable metabolic effects. *P. Natl. Acad. Sci. U. S. A.* **103**, 15675–15680
 28. Tsurutani, Y., Fujimoto, M., and Yokote, K. (2009) Myostatin (MSTN) inhibits adipogenesis and high-fat induced obesity via smad3: a possibility of crosstalk between muscle and adipose tissue. *Diabetes* **58**, A436–A437
 29. Fournier, B., Murray, B., Gutzwiller, S., Marcaletti, S., Marcellin, D., Bergling, S., Brachat, S., Persohn, E., Pierrel, E., Bombard, F., Hatakeyama, S., Trendelenburg, A. U., Morvan, F., Richardson, B., Glass, D. J., Lach-Trifileff, E., and Feige, J. N. (2012) Blockade of the activin receptor IIB activates functional brown adipogenesis and thermogenesis by inducing mitochondrial oxidative metabolism. *Mol. Cell Biol.* **32**, 2871–2879
 30. Kim, W. K., Choi, H. R., Park, S. G., Ko, Y., Bae, K. H., and Lee, S. C. (2012) Myostatin inhibits brown adipocyte differentiation via regulation of Smad3-mediated β -catenin stabilization. *Int. J. Biochem. Cell Biol.* **44**, 327–334
 31. Schulz, T. J., Huang, T. L., Tran, T. T., Zhang, H. B., Townsend, K. L., Shadrach, J. L., Cerletti, M., McDougall, L. E., Giorgadze, N., Tchekonia, T., Schrier, D., Falb, D., Kirkland, J. L., Wagers, A. J., and Tseng, Y. H. (2011) Identification of inducible brown adipocyte progenitors residing in skeletal muscle and white fat. *Proc. Natl. Acad. Sci. U. S. A.* **108**, 143–148
 32. Yadav, H., Quijano, C., Kamaraju, A. K., Gavrilova, O., Malek, R., Chen, W. P., Zervas, P., Duan, Z. G., Wright, E. C., Stuelten, C., Sun, P., Lonning, S., Skarulis, M., Sumner, A. E., Finkel, T., and Rane, S. G. (2011) Protection from obesity and diabetes by blockade of TGF- β /Smad3 signaling. *Cell Metab.* **14**, 67–79
 33. Wen, Y. F., Bi, P. P., Liu, W. Y., Asakura, A., Keller, C., and Kuang, S. H. (2012) Constitutive Notch activation upregulates Pax7 and promotes the self-renewal of skeletal muscle satellite cells. *Mol. Cell Biol.* **32**, 2300–2311
 34. Liu, W. Y., Wen, Y. F., Bi, P. P., Lai, X. S., Liu, X. S., Liu, X. Q., and Kuang, S. H. (2012) Hypoxia promotes satellite cell self-renewal and enhances the efficiency of myoblast transplantation. *Development* **139**, 2857–2865
 35. Liu, W. Y., Liu, Y. Q., Lai, X. S., and Kuang, S. H. (2012) Intramuscular adipose is derived from a non-Pax3 lineage and required for efficient regeneration of skeletal muscles. *Dev. Biol.* **361**, 27–38

36. Shan, T., Liu, W., and Kuang, S. (2013) Fatty acid binding protein 4 expression marks a population of adipocyte progenitors in white and brown adipose tissues. *FASEB J.* **27**, 277–287
37. Guo, T. Q., Jou, W., Chanturiya, T., Portas, J., Gavrilova, O., and McPherron, A. C. (2009) Myostatin inhibition in muscle, but not adipose tissue, decreases fat mass and improves insulin sensitivity. *PLoS One* **4**, e4937
38. Kelly, D. P. (2012) Medicine. Irisin, light my fire. *Science* **336**, 42–43
39. Koncarevic, A., Kajimura, S., Cornwall-Brady, M., Andreucci, A., Pullen, A., Sako, D., Kumar, R., Grinberg, A. V., Liharska, K., Ucran, J. A., Howard, E., Spiegelman, B. M., Seehra, J., and Lachey, J. (2012) A novel therapeutic approach to treating obesity through modulation of TGF β signaling. *Endocrinology* **153**, 3133–3146
40. Guo, T. Q., Bond, N. D., Jou, W., Gavrilova, O., Portas, J., and McPherron, A. C. (2012) Myostatin inhibition prevents diabetes and hyperphagia in a mouse model of lipodystrophy. *Diabetes* **61**, 2414–2423
41. Mehran, A. E., Templeman, N. M., Brigidi, G. S., Lim, G. E., Chu, K. Y., Hu, X., Botezelli, J. D., Asadi, A., Hoffman, B. G., Kieffer, T. J., Banji, S. X., Clee, S. M., and Johnson, J. D. (2012) Hyperinsulinemia drives diet-induced obesity independently of brain insulin production. *Cell Metab.* **16**, 723–737
42. LeBrasseur, N. K., Schelhorn, T. M., Bernardo, B. L., Cosgrove, P. G., Loria, P. M., and Brown, T. A. (2009) Myostatin inhibition enhances the effects of exercise on performance and metabolic outcomes in aged mice. *J. Gerontol. A Biol. Sci. Med. Sci.* **64**, 940–948
43. Murphy, K. T., Koopman, R., Naim, T., Leger, B., Trieu, J., Ibebunjo, C., and Lynch, G. S. (2010) Antibody-directed myostatin inhibition in 21-mo-old mice reveals novel roles for myostatin signaling in skeletal muscle structure and function. *FASEB J.* **24**, 4433–4442
44. Zhang, C., McFarlane, C., Lokireddy, S., Bonala, S., Ge, X., Masuda, S., Gluckman, P. D., Sharma, M., and Kambadur, R. (2011) Myostatin-deficient mice exhibit reduced insulin resistance through activating the AMP-activated protein kinase signalling pathway. *Diabetologia* **54**, 1491–1501
45. Hennebry, A., Berry, C., Siriott, V., O’Callaghan, P., Chau, L., Watson, T., Sharma, M., and Kambadur, R. (2009) Myostatin regulates fiber-type composition of skeletal muscle by regulating MEF2 and MyoD gene expression. *Am. J. Physiol. Cell Physiol.* **296**, C525–C534
46. Girgenrath, S., Song, K., and Whittemore, L. A. (2005) Loss of myostatin expression alters fiber-type distribution and expression of myosin heavy chain isoforms in slow- and fast-type skeletal muscle. *Muscle Nerve* **31**, 34–40
47. Jorgensen, S. B., Richter, E. A., and Wojtaszewski, J. F. (2006) Role of AMPK in skeletal muscle metabolic regulation and adaptation in relation to exercise. *J. Physiol.* **574**, 17–31
48. Lee-Young, R. S., Canny, B. J., Myers, D. E., and McConell, G. K. (2009) AMPK activation is fiber type specific in human skeletal muscle: effects of exercise and short-term exercise training. *J. Appl. Physiol.* **107**, 283–289
49. Glass, D. J. (2010) PI3 kinase regulation of skeletal muscle hypertrophy and atrophy. *Curr. Top. Microbiol. Immunol.* **346**, 267–278
50. Argiles, J. M., Orpi, M., Busquets, S., and Lopez-Soriano, F. J. (2012) Myostatin: more than just a regulator of muscle mass. *Drug Discov. Today* **17**, 702–709

*Received for publication December 6, 2012.
Accepted for publication January 22, 2013.*